https://doi.org/10.5194/egusphere-2026-4415
Preprint. Discussion started: 11 August 2026

Long-Term Satellite Analysis of Summer Heatwaves and Heat Vulnerability in Romania (2000–2025)

Claudiu-Valeriu Angearu, National Meteorological Administration, Bucharest, Romania
Florinela Georgescu, National Meteorological Administration, Bucharest, Romania
Anişoara Irimescu, National Meteorological Administration, Bucharest, Romania
Denis Mihăilescu, National Meteorological Administration, Bucharest, Romania
Vasile Crăciunescu, National Meteorological Administration, Bucharest, Romania
Marian Neagul, Institute for Advanced Environmental Research, University of Timisoara, Timisoara, Romania
*corresponding email: anisoara.irimescu@meteoromania.ro

Abstract

Heatwaves represent one of the most significant climate-related hazards affecting human health, ecosystems, and socioeconomic activities. This study presents the first multi-decadal, national-scale assessment of summer heatwaves and heat vulnerability in Romania using a 26-year archive (2000–2025) of MODIS Land Surface Temperature (LST) integrated with official meteorological warnings and high-resolution population-grid data. Daily satellite observations were processed to analyze long-term trends, anomalies, and consecutive hot days. A 1-km Heat Vulnerability Index (HVI) was developed by fusing satellite-derived thermal hazard data, cumulative heat-warning severity, population density, and demographic sensitivity.

The results indicate a severe and widespread intensification of summer thermal conditions across Romania, with August exhibiting the strongest surface warming trend (1.76°C decade^{-1}), followed by July (0.82°C decade^{-1}), and a seasonal average increase of 0.84°C decade^{-1}. Maximum LST frequently exceeded 50°C in the southern lowlands during the most extreme summers on record (2007, 2012, 2022, 2024, and 2025), with 2024 registering a record-breaking 56 heatwave days. The southern lowlands and the Bucharest metropolitan area emerged as the principal national hotspots of heat-related risk. Nationally, over 3.15 million inhabitants (16.5% of the total population) reside in areas classified under high and very high vulnerability classes, with Bucharest alone concentrating 1.82 million vulnerable citizens. The proposed framework provides an operational, high-utility tool for geographic screening, directly supporting evidence-based public health interventions and climate adaptation strategies.

Keywords: Remote sensing climatology; Environmental health screening; Spatial risk allocation; Population exposure; Thermal anomalies; MODIS Aqua/Terra.

Introduction

Heat waves represent one of the most hazardous climate-related extremes because they affect human health, agriculture, water resources, energy demand and ecosystem functioning. Their impacts are expected to intensify under ongoing climate change, increasing the need for effective monitoring, early-warning systems and adaptation strategies.

There is a wide range of definitions of heatwaves, depending on their frequency, intensity, duration, and on thresholds that vary according to the climatic characteristics of different geographical regions. In general, heatwaves are identified by thermal anomalies above a defined threshold, persisting for several consecutive days. The threshold may take the form of a fixed temperature value or a percentile-based threshold defined in relation to the temperature distribution of a specific location (Bojariu et al., 2021).

According to WMO Task Team (2018), a heatwave can be defined as "*a period of marked unusual hot weather (maximum, minimum and daily average temperature) over a region persisting at least three consecutive days during the warm period of the year based on local (station-based) climatological conditions, with thermal conditions recorded above given thresholds*".

Heatwaves are generally defined based on the persistence of both daytime and nighttime high temperatures. However, many countries have adopted local criteria for issuing heatwave-related warnings. In the Netherlands, Belgium, or Luxembourg, a heatwave is defined as a period of at least five consecutive days with maximum temperatures above 25°C, whereas in Denmark it is defined as a period of at least three consecutive days with mean maximum temperatures above 28°C across more than half the country. In Romania, however, the 25°C

https://doi.org/10.5194/egusphere-2026-4415
Preprint. Discussion started: 11 August 2026

threshold only represents the normal thermal limit of a summer day (Dima et al., 2016). Other definitions used by meteorological services include: *"a period of abnormally hot weather lasting generally more than two days.*

Heatwaves can occur with or without high humidity" (US National Weather Service), *"a period of abnormally hot and unusually humid weather. Usually, a heatwave lasts two or more days"* (NOAA), and *"a prolonged period of hot weather relative to expected conditions at that time of year and in the area concerned, where humidity may also be high"* (Met Office) (Bunting et al., 2024).

Since there is no universal temperature threshold that defines extreme heat, heatwaves are defined in relation to the local climate. The same meteorological conditions may constitute a heatwave in one region but not in another, and in order to understand the impacts of extreme temperatures on human comfort or health, nighttime temperatures are just as important as daytime ones (WMO & WHO, 2015). Therefore, this approach to defining heatwaves is relevant for thermal climate hazards with impacts on human health and comfort (Mărășoiu, 2015; Croitoru et al., 2018). Nonetheless, non-climatological variables such as exposure, vulnerability, population, and land use/land cover are still seldom incorporated into heatwave definitions (Bunting et al., 2024).

In relation to local climatic conditions, a heatwave is a period of excessively hot weather. Thus, in regions with colder climates, temperatures may be recorded over several consecutive days that are anomalous relative to the normal thermal regime of that region and period, suggesting the occurrence of a heatwave. Meteorologists generally associate such episodes with anticyclonic atmospheric patterns, which are characterized by prolonged periods of clear skies and elevated temperatures in the atmospheric boundary layer (Barriopedro et al., 2011).

In the 21st century, **Europe** experienced the devastating 2003 summer heatwave, which caused tens of thousands of fatalities due to extreme temperatures and prolonged thermal discomfort (Ionita et al., 2021; Nagavciuc et al., 2022; Ionita et al., 2024; Martins et al., 2024).

In **Romania**, intense and persistent heatwaves have become increasingly frequent in recent decades, as illustrated by the events of 2007, 2012, 2015, 2017, and 2021 (Croitoru et al., 2016; Sfică et al., 2017; Piticar et al., 2018; Bojariu et al., 2021), followed by the last three summers (2022, 2023, 2024). Romanian heatwaves can be generated by tropical air advections, which lead to strong positive temperature anomalies relative to climatological norms and sometimes even new record values (Dima et al., 2016).

In temperate regions, the highest daily maximum air temperatures are recorded from mid-June until late August. When both daily maximum and minimum temperatures are high, and the diurnal amplitude is reduced, this phenomenon is referred to as a hot day (heatwave) in Romania. In such cases, daytime maximum temperatures reach or exceed 35°C, while nighttime minimum temperatures remain around or above 20°C (Mărășoiu, 2015; Dima et al., 2016; Croitoru et al., 2018).

Heatwaves in Romania are predominantly associated with the advection of continental tropical air masses originating from North Africa or the Arabian Peninsula (Dima et al., 2016). These warm-air intrusions occur under persistent anticyclonic circulation conditions, characterized by the extension of the Azores High over southeastern Europe and dominant southwesterly to northwesterly flow in the middle troposphere. Such large-scale synoptic configurations promote prolonged atmospheric stability, enhanced surface heating, and the persistence of extreme high-temperature events across the country.

The spatial distribution of heat waves is not homogeneous across Romania. The southern part of the country is the most frequently affected region, while mountainous areas experience substantially fewer and shorter heat-wave episodes owing to altitude and regional climatic influences (Barbu et al. 2014; Dima et al., 2016).

https://doi.org/10.5194/egusphere-2026-4415
Preprint. Discussion started: 11 August 2026

Recent research has also highlighted the increasing importance of heatwave monitoring in Romania. Cheval et al. (2025) analysed the characteristics of urban heatwaves in 41 Romanian cities using air temperature observations, describing their magnitude, duration, frequency, and projected future evolution under climate change scenarios. Their results indicate that Romanian cities will experience increasingly frequent and intense heatwaves, emphasizing the need for region-specific adaptation strategies and continuous monitoring.

Climate projections indicate that both the frequency and duration of heatwaves will increase across Romania under the RCP4.5 and RCP8.5 scenarios, with the strongest changes expected in southern regions, leading to greater population exposure to extreme heat. Mean heatwave duration is projected to increase by approximately 30–50% under RCP4.5 and by 50–70% under RCP8.5 over southern Romania (Antonescu et al. 2023). This long-term trend is further corroborated by recent observational data from the hottest summers on record, specifically 2023 and 2024, which demonstrated an unprecedented proliferation of compound hot-dry extremes and extended thermal blocks across Eastern Europe (Ionita et al., 2025; Antonescu & Ioniță, 2024). Furthermore, recent modeling efforts have emphasized that the intersection between expanding built-up urban footprints and these intensified synoptic events triggers severe microclimatic disruptions, causing surface urban heat islands to peak in intensity during nighttime cycles (Cheval et al., 2025; Gabrian et al., 2025). While recent institutional initiatives, such as the public platform Romania Heat Atlas (2026), have significantly advanced the mapping of physical heatwave dynamics and indoor-outdoor thermal comfort indicators like the Wet Bulb Global Temperature across major Romanian cities, these open-access frameworks focus predominantly on spatializing climatological hazard thresholds at localized urban scales. The present study addresses a critical methodology gap by conceptualizing heat risk at a continuous national scale. By integrating multi-decadal, dual-satellite MODIS-derived thermal exposure with high-resolution census statistics, we model population density and structural demographic sensitivity into a unified, geospatial 1-km Heat Vulnerability Index (HVI) spanning the entire country.

Understanding the atmospheric circulation patterns responsible for heat-wave formation is essential for improving weather forecasting, early-warning systems and climate adaptation. Consequently, identifying areas where intense heat coincides with high population exposure and demographic vulnerability represents a key step toward reducing heat-related risks (Sfica et al., 2017).

Heatwaves can be analyzed using a single **meteorological parameter** (e.g., maximum air temperature) or through more complex approaches combining ground-based meteorological station data with indices derived from **satellite imagery**. Thermal infrared (TIR) satellite data can be used to estimate diurnal land surface temperature amplitudes, assess thermal stress, and support public health warning systems.

In Romania, the spatial distribution of air temperature is strongly controlled by altitude. As illustrated in Figure 1, the annual mean daily **maximum air temperature** during the warm season exhibits a pronounced altitudinal gradient, with the highest values consistently observed below 200 m and progressively lower temperatures towards the highest mountain areas. Despite these marked differences, a coherent warming trend is evident across all 13 altitudinal zones during the 2000–2025 period, indicating that recent climate warming affects not only lowland regions but also high-elevation environments. Several exceptionally warm years, including 2007, 2012, 2015 and the recent period 2022–2025, stand out across nearly all elevation belts, suggesting that heat extremes have become increasingly widespread rather than being restricted to low-altitude regions. These findings indicate a growing potential for heat-related impacts across Romania and further highlight the need for spatially explicit assessments of heat hazard, exposure and population vulnerability.

https://doi.org/10.5194/egusphere-2026-4415
Preprint. Discussion started: 11 August 2026

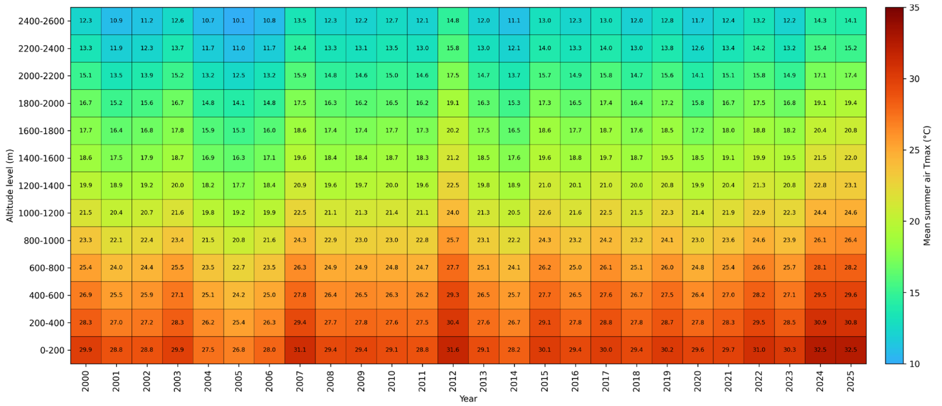

Figure 1. Spatiotemporal evolution of annual mean daily maximum air temperature across Romania

Land Surface Temperature (**LST**) is a useful indicator for estimating the surface energy balance and greenhouse effect, since both influence numerous terrestrial biophysical processes. LST varies rapidly in space and time, mainly due to the diurnal and annual cycles of the Earth. Information regarding the temporal dynamics of LST (seasonal, annual, and interannual) is essential for determining energy fluxes between the atmosphere and the land surface. Numerous studies have analyzed heatwaves using satellite-derived LST indices from different sensors (e.g., Landsat in Buscail et al., 2012; MODIS in Zaitchik et al., 2006; Zoran et al., 2011; Gusso et al., 2014; NOAA-AVHRR in Dousset et al., 2011).

Data and Methods

1. Data Used

The analysis of summer temperatures and heatwaves across Romania was carried out using the daily Land Surface Temperature and Emissivity products MYD11A1 (Collection 6.1) derived from Aqua MODIS for the period 2002–2025, complemented by MOD11A1 (Terra MODIS) for 2000–2001, prior to the operational availability of Aqua.

The daytime Aqua overpass over Romania occurs at approximately 13:30–15:10 local time, close to the period of maximum daytime surface heating, whereas Terra acquires observations earlier, at approximately 10:30–12:10 local time. The daily LST and emissivity products are generated at a spatial resolution of 1 km using the generalized split-window algorithm, with a reported accuracy of approximately ±1 K under clear-sky conditions.

It should be noted that land surface temperature (LST) differs fundamentally from near-surface air temperature (Tmax), and therefore discrepancies are expected between values measured at meteorological stations and those retrieved from satellite observations. These differences arise from several factors: (i) the measurement level, as air temperature is recorded at 2 m above the ground whereas satellite sensors measure the radiometric temperature of the Earth's surface (e.g., vegetation canopy, rooftops, bare soil or asphalt); (ii) differences in land-cover and surface characteristics, which strongly influence the surface energy balance; and (iii) the observation time, since MODIS daytime overpasses Romania between approximately 10:30 and 12:10 UTC, while meteorological stations report the daily maximum air temperature, which generally occurs later in the afternoon. Additionally, while thermal infrared remote sensing is inherently subject to clear-sky bias, synoptic heatwave formation in this geographical region is strongly linked with stable, anticyclonic configurations. Given that extreme thermal events predominantly develop under low-cloud atmospheric blocks, this sampling constraint exerts a negligible structural impact on the integrity of the peak land surface temperature climatology. Despite these differences, LST and air temperature are closely related under clear-sky conditions and complementary analyses, including correlation statistics and LST–Tmax

https://doi.org/10.5194/egusphere-2026-4415
Preprint. Discussion started: 11 August 2026

differences, were performed to evaluate their relationship and to quantify the additional heating of the land surface during heat-wave events.

County-level data on the percentage of households equipped with at least one air conditioning unit (INS, 2021) were linked to the corresponding county polygons and compared with the classified Heat Vulnerability Index (HVI). This analysis enabled the identification of counties characterized by high heat vulnerability and low air conditioning coverage, highlighting areas with potentially limited adaptive capacity to extreme heat.

An overview of the datasets used, data processing steps, and the main methodological framework adopted in this study is presented in the workflow shown in Figure 2.

2. Methods

Daily MODIS Land Surface Temperature (LST) data for Romania were processed and downloaded using the Google Earth Engine platform through a Python-based workflow, followed by post-processing and spatial analyses in RStudio. The analyses included long-term trends, anomalies, annual maximum LST, monthly averages, and the number of consecutive days exceeding predefined LST thresholds.

In addition, daily maximum air temperature (Tmax) observations (at 1 km spatial resolution, extracted from *Romanian National Meteorological Administration (ANM) archive*) were incorporated to evaluate the relationship between satellite-derived LST and near-surface air temperature. Correlation analyses and statistical comparisons were performed to quantify the agreement between the two datasets and to assess the magnitude by which land surface temperature exceeds maximum air temperature during heat-wave conditions.

Furthermore, official heat-warning records (yellow, orange and red warning levels) issued by the Romanian National Meteorological Administration and the Eurostat 2021 population grid (Tucci et al., 2026), including total population and the population aged ≥65 years, were integrated to develop a **1-km Heat Vulnerability Index (HVI)**.

The selection of the cohort aged ≥65 years as the primary indicator for demographic vulnerability reflects the structural breakdown of the latest national census database, which aggregates population statistics into three macro-age categories: under 15 years, 15 to 64 years, and 65 years and over. From a biometeorological perspective, this senior cohort represents the segment of the population with the highest physical vulnerability to extreme thermal stress due to age-related thermoregulatory degradation and a higher prevalence of baseline cardiovascular conditions. Utilizing this standardized age threshold ensures strict alignment with official demographic reporting while capturing the core spatial distribution of the most heat-sensitive population group across Romania. The HVI combines satellite-derived land surface temperature, cumulative heat-warning severity, population exposure and demographic vulnerability. All variables were robustly normalized using the 2nd and 98th percentiles, integrated using an equal-weight approach, and classified into five fixed vulnerability classes (Very Low, Low, Moderate, High and Very High), providing a comprehensive spatial assessment of heat-related vulnerability across Romania.

The adoption of an equal-weighting scheme represents a well-established and transparent benchmark approach in macro-scale vulnerability mapping. In national-scale assessments spanning geographically and socio-economically heterogeneous regions, assigning identical baseline weights eliminates subjective or localized structural biases that often arise from statistical weighting techniques like Principal Component Analysis, which can over-optimize for specific urban environments at the expense of regional accuracy. This operational neutrality ensures that the index functions effectively as a straightforward screening tool, making its computational framework highly reproducible for public health administrators and spatial planners tracking national climate risk allocation.

https://doi.org/10.5194/egusphere-2026-4415
Preprint. Discussion started: 11 August 2026

Furthermore, technological adaptive capacity—represented by county-level household air conditioning ownership from the 2021 census—was intentionally excluded from the pixel-level algebraic calculation of the HVI. Because socioeconomic and infrastructure statistics are commercially and administratively aggregated at broad county levels, integrating them directly into a 1-km raster matrix would trigger severe ecological fallacies, artificially smoothing out localized urban-rural risk boundaries. Instead, this layer is treated strictly as a regional macro-contextual overlay within the discussion framework to isolate systemic adaptation deficits without corrupting the high-resolution grid dynamics.

The Romanian colour-coded heat warning system follows the European MeteoAlarm (European Multi-service Meteorological Awareness, EMMA) framework (EUMETNET, 2024), which was adopted by the Romanian National Meteorological Administration (NMA) in 2008. According to the national warning methodology (Joint Order No. 245/2012), yellow, orange, and red warnings are defined based on maximum air temperature, the Temperature–Humidity Index (THI), and the persistence of heatwave conditions. In general, the corresponding maximum air temperature thresholds are 33–36°C (yellow), 37–39°C (orange), and ≥40°C (red). Consequently, official yellow, orange, and red heat warnings are available only from 2007 onwards, rendering these operational alerts structurally unavailable for the early years of our baseline. To resolve this and ensure chronological homogeneity across the entire multi-decadal study period, the utilization of a fixed threshold of 35°C was implemented to identify heatwave days prior to 2007. In the Romanian climatological nomenclature, an air temperature reaching or exceeding 35°C officially defines a tropical, scorching day. Therefore, applying this historical physiological threshold as a baseline proxy before the operational rollout of the Meteoalarm-aligned system establishes a mathematically consistent and structurally continuous timeline, ensuring that long-term trends reflect true atmospheric evolution rather than shifts in institutional reporting protocols.

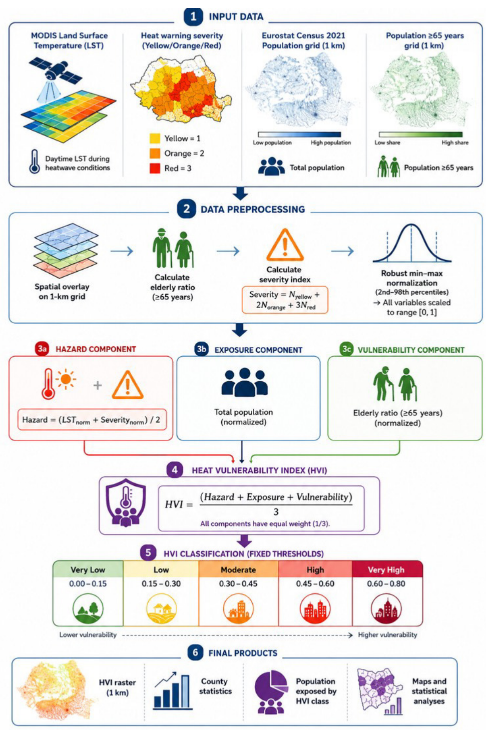

Figure 2 Workflow used for calculating the Heat Vulnerability Index (HVI)

https://doi.org/10.5194/egusphere-2026-4415
Preprint. Discussion started: 11 August 2026

The Heat Vulnerability Index was developed to quantify the spatial distribution of population vulnerability to heat-related impacts by integrating three equally important dimensions: **hazard**, **exposure**, and **demographic vulnerability**. The index was calculated on a 1-km population grid covering Romania using an equal-weighting approach, which avoids subjective weighting assumptions and provides a transparent and reproducible framework.

The hazard component was defined as the average of two normalized variables: (i) mean land surface temperature (LST) derived from satellite observations during heatwave conditions and (ii) the cumulative heat-warning severity index calculated from official meteorological warnings. The severity index was computed by assigning a weight of 1 to yellow warnings, 2 to orange warnings, and 3 to red warnings, according to:

$$Severity = Nyellow + 2Norange + 3Nred$$

where *Nyellow*, *Norange*, and *Nred* represent the cumulative number of warnings of each category over the study period.

The exposure component was represented by the total resident population within each 1-km grid cell, whereas demographic vulnerability was expressed as the proportion of residents aged 65 years and older. Before integration, all variables were normalized to a common range using robust min-max normalization based on the 2nd and 98th percentiles to reduce the influence of extreme values. The normalized hazard component was calculated as:

$$Hazard = \frac{\text{LST norm} + \text{Severity norm}}{2}$$

Finally, the Heat Vulnerability Index was computed as:

$$\text{HVI} = \frac{\text{Hazard} + \text{Exposure} + \text{Vulnerability}}{3}$$

where:

- **Hazard** = normalized thermal hazard,
- **Exposure** = normalized total population,
- **Vulnerability** = normalized proportion of population aged ≥65 years.

All three components received identical weights (1/3), following the principle that hazard, exposure, and vulnerability contribute equally to heat-related risk in the absence of objective evidence supporting differential weighting. For mapping and statistical analyses, the continuous HVI values were classified into five fixed vulnerability classes using predefined thresholds:

Table 1. HVI classification

HVI	Vulnerability class
0.00–0.15	*Very Low*
0.15–0.30	*Low*
0.30–0.45	*Moderate*
0.45–0.60	*High*
0.60–0.80	*Very High*

Results

A. Analysis of Summer LST Values (2000–2025)

The LST heatmap (Fig. 3) shows an increasing trend in the frequency of days with high temperatures. The most recent years (2020–2025) indicate a notable rise in days with temperatures exceeding 35°C, highlighting both the increasing intensity and frequency of heatwaves. In addition to the recent hot years, 2000, 2003, 2007, 2012, and 2015 also stand out. These years recorded consecutive days with LST values above 38°C, coinciding with drought events reported in the literature, which further demonstrates the correlation between high temperatures and stress on water resources and agriculture.

https://doi.org/10.5194/egusphere-2026-4415
Preprint. Discussion started: 11 August 2026

Regarding the months with the highest LST values, July consistently recorded the maximum peaks, followed by August. The highest monthly mean LST was in July 2007 (35.4°C), followed by July 2025 (34.96°C), August 2024 (34.7°C), July 2012 (34.6°C), and July 2024 (33.9°C) (Fig. 3). Monthly average LST values indicate that summer **2025** was the hottest on record, with a mean LST of 33.43°C, followed by summer **2024** (32.83°C), **2012** (32.75°C) and **2007** (32.43°C).

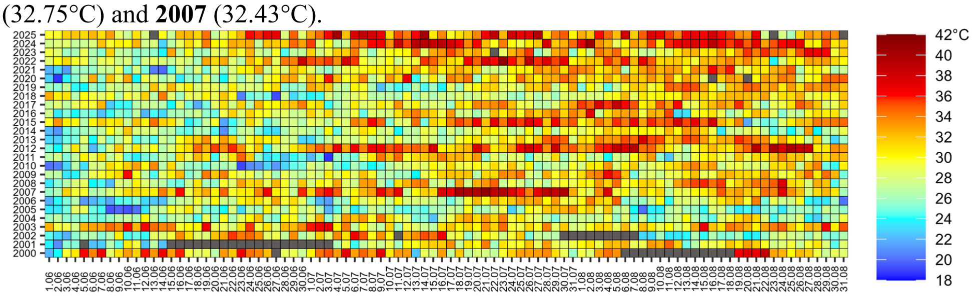

Figure 3. LST Values in Romania During the Summer Season, 2000–2025

The **comparison** between MODIS LST and daily maximum air temperature reveals a robust linear relationship, confirming that both variables respond consistently to heatwave conditions. However, LST systematically exceeds Tmax, with an average difference of 2.75°C, reflecting the more rapid heating of the land surface relative to the overlying air. This behaviour is observed across all LST classes, suggesting that the LST–air temperature difference remains relatively stable even under the most extreme thermal conditions (Fig. 4).

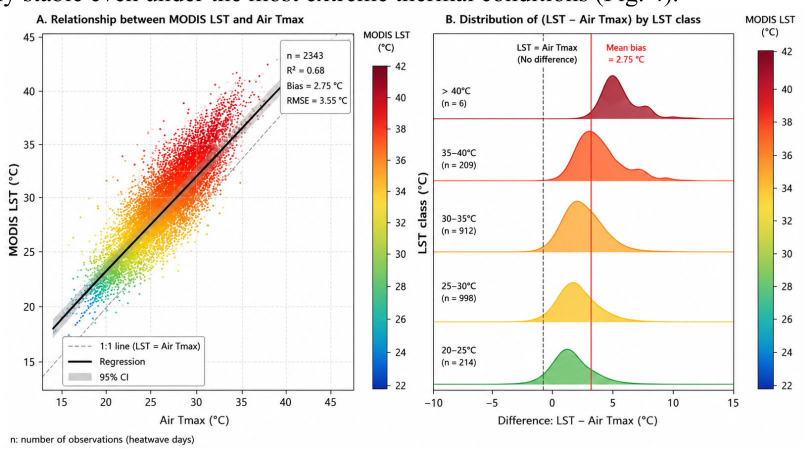

Figure 4. MODIS LST and Air Tmax comparison during summer days (2000-2025)

The spatial distribution of monthly **LST anomalies** in Romania (2000–2025) (Figure S1) reveals distinct interannual variability, with strong positive anomalies occurring in years marked by extreme heat events. **July 2007** stands out with widespread anomalies exceeding +10°C across southern and eastern Romania, reflecting one of the most severe heatwaves in recent decades. Similarly, August 2012 and August 2024 display large areas with high anomalies, particularly in the Romanian Plain and Dobrogea, confirming the intensity of heatwaves during these periods.

By contrast, years such as 2005, 2014, and 2018 show predominantly negative anomalies (−5°C to −10°C), indicating cooler-than-average summers. Spatially, the highest anomalies are consistently concentrated in lowland regions (the Romanian Plain, Dobrogea Plateau, and

https://doi.org/10.5194/egusphere-2026-4415
Preprint. Discussion started: 11 August 2026

western plains), while more moderate values are observed in Transylvania (center of the country) and mountainous areas, where altitude mitigates extreme surface heating.

The ranking of monthly LST anomalies in Romania for the period 2000–2025 highlights several extreme events. The most pronounced anomaly was recorded in **July 2007** (+5.3°C). The following values correspond to July 2025, July 2024 and August 2012, associated with intense and long-lasting heatwaves.

Linear **trends** in mean monthly summer LST reveal a marked intensification of surface warming across Romania during the 2000–2025 period, although the magnitude and spatial extent of these changes differ considerably among the summer months (Fig. 5). June exhibited relatively weak and spatially heterogeneous trends, with localized areas of slight cooling, resulting in a near-zero mean trend (−0.07 °C decade^{-1}). In contrast, July and August were characterized by widespread positive trends across almost the entire country, with mean warming rates of 0.82 and 1.76 °C decade^{-1}, respectively. August displayed the strongest and most spatially homogeneous warming pattern, with positive trends affecting approximately 99% of the study area, while July showed warming over 93% of Romania. The seasonal (JJA) trend integrated these monthly patterns and indicated an average increase of 0.84 °C decade^{-1}, with **positive trends** covering approximately 97% of the country. These findings indicate that recent summer warming has become increasingly widespread, particularly during the peak summer months, reinforcing the observed intensification of heatwave conditions across Romania.

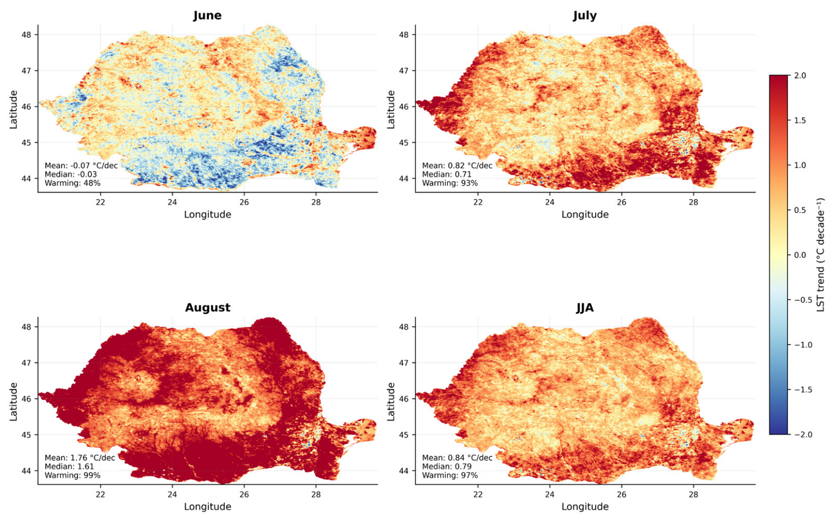

Figure 5. Summer LST trend in Romania by month and season, reference period 2000–2025

Based on the **number of consecutive days** with different **LST** thresholds (**35°C**, **40°C**, **45°C**, **50°C** – Fig. S2), high-incidence areas were identified in the Romanian Plain (especially the central part) and Dobrogea, while moderate to low values occurred in Transylvania, and heatwaves were practically absent in mountain areas and the Danube Delta. As the LST threshold increases, both the extent of affected areas and the number of consecutive days decrease. Thus, while the number of consecutive days with **LST > 35°C** reaches a maximum of more than 16 days in July and August, at the **LST > 40°C** threshold the frequency and spatial extent of high temperatures decrease considerably.

For the **50°C** threshold, extreme heat was observed especially in July, in the Romanian Plain and Dobrogea Plateau, later peaking in August with up to 11 consecutive days in the

https://doi.org/10.5194/egusphere-2026-4415
Preprint. Discussion started: 11 August 2026

Oltenia Plain. At the highest threshold (**LST > 55°C**), extreme heat appeared only in July and August, mainly in the Teleorman Plain, with sequences of up to 10 days.

Analysis of the **years with the maximum number of consecutive** days above LST > 35°C (Fig. S3) revealed a territorial distribution of heatwave intensity, with the largest spatial extents recorded in 2007, 2012, 2015, and 2022. At higher thresholds (LST > 40°C, 50°C, 55°C), the extent of extremely hot areas decreased, clearly highlighting the most extreme years (2007, 2012, 2015, 2022, 2024).

B. Analysis of Heatwaves Based on LST Data

The temporal evolution of heatwave days reveals a pronounced increase in the frequency, persistence, and thermal intensity of extreme summer conditions across Romania during the 2000–2025 period (Fig. 6). **Heatwave episodes** were defined as sequences of at **least three consecutive days** associated with official yellow, orange, or red heat warnings issued by NMA.

During the study period, the **highest number** of heatwave days was recorded in **2024** (56 days), followed by 2025 (45 days), 2022 (39 days), 2012 (37 days), 2023 (36 days), and 2021 (34 days). While only isolated and relatively short heatwave episodes occurred during the early 2000s, their frequency and duration increased substantially after 2020. Moreover, the predominance of orange and red cells during recent summers indicates that these events were increasingly associated with high mean MODIS LST values, frequently exceeding 35°C and, in several cases, 40°C. The longer uninterrupted sequences of heatwave days observed in 2021–2025 further demonstrate an increase in the persistence of extreme thermal conditions, highlighting the growing severity of summer heatwaves across Romania.

The distribution of heatwave days by mean LST class reveals that most heatwave events occurred within the 32–34°C and 34–36°C intervals, accounting for 118 and 108 days, respectively (Fig. S5). A substantial number of heatwave days were also recorded within the 30–32°C (73 days) and 36–38°C (71 days) classes, indicating that the majority of heatwave conditions were associated with moderate to high surface temperatures. In contrast, very high LST values were considerably less frequent, with only 31 days recorded in the 38–40°C class and six days exceeding 40°C. Heatwave days associated with mean LST below 30°C were rare, representing less than 7% of the total. Overall, the distribution demonstrates that Romanian heatwaves are predominantly characterized by mean LST values between **32** and **36°C**, whereas extremely high surface temperatures (>40°C) occur only during the most severe events.

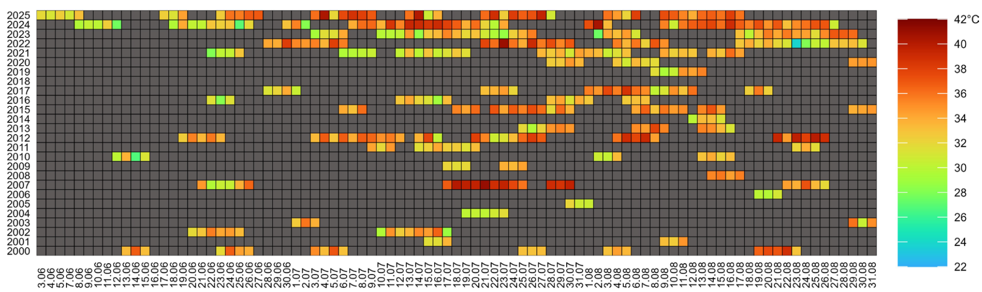

Figure 6. Heatwave Days During the Period 2000–2025 (LST mean values for Romania)

The combined analysis of mean LST and heatwave-warning days across the 13 altitudinal zones reveals a pronounced elevation-dependent pattern throughout the 2000–2025 period (Fig. 7). Mean LST decreases progressively with increasing altitude, with the highest temperatures consistently recorded below 200 m and the lowest values observed above 2200 m. Despite this strong altitudinal gradient, recent years exhibit a clear increase in LST across all elevation bands, indicating that summer warming is not restricted to lowland regions.

https://doi.org/10.5194/egusphere-2026-4415
Preprint. Discussion started: 11 August 2026

The number of heatwave-warning days also increased substantially over time, particularly after 2020, with the largest totals recorded during 2024 and 2025. Although warning days occurred predominantly at lower elevations, their presence at higher altitudes during recent years demonstrates the upward expansion of heatwave conditions.

Furthermore, the composition of warning levels shifted towards a greater contribution of orange and red warnings during the most recent summers, reflecting an increase not only in the frequency but also in the severity of heatwave events across Romania.

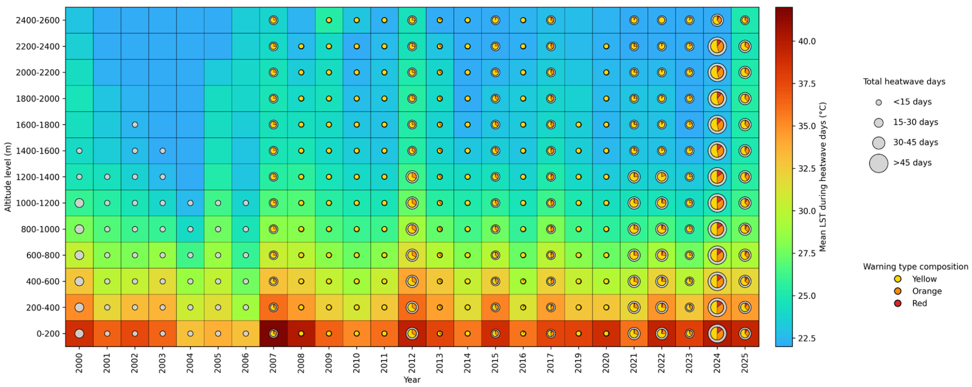

Figure 7. Mean LST and heatwaves warning days by altitude level

The spatial distribution of **maximum** LST recorded during heatwave events between 2000 and 2025 reveals a pronounced geographical pattern across Romania (Fig. 8). The highest maximum LST values (>53°C, locally exceeding 57°C) were consistently observed in the **southern** and **southeastern lowlands**, particularly across the Romanian Plain, Bărăgan Plain, and Dobrogea. Elevated maximum LST values (48–57°C) also extended into the western lowlands, including the Banat and Crișana plains.

In contrast, the lowest maximum LST values (<36°C) were concentrated in the Carpathian Mountains and the highest mountain ranges, where altitude and dense forest cover contribute to substantially lower surface temperatures. Intermediate values (36–44°C) characterized the hilly and plateau regions surrounding the mountain chain, reflecting the strong influence of topography on the spatial distribution of surface thermal extremes.

Overall, the map highlights a clear altitudinal and physiographic control on maximum LST, with low-elevation regions exhibiting the greatest susceptibility to extreme surface heating during heatwave events. The persistence of these spatial hotspots throughout the study period suggests that southern and southeastern Romania represent the most thermally vulnerable regions, whereas mountainous areas act as persistent thermal refugia during extreme summer conditions.

Representative examples of the most intense **heatwave days** during the 2000–2025 period are presented in Figure S4 to illustrate the spatial distribution of extreme LST. Although the summers of 2007, 2012, 2022, 2024, and 2025 were all characterized by extensive areas of exceptionally high LST, only selected days are shown to highlight the spatial variability of these events.

https://doi.org/10.5194/egusphere-2026-4415
Preprint. Discussion started: 11 August 2026

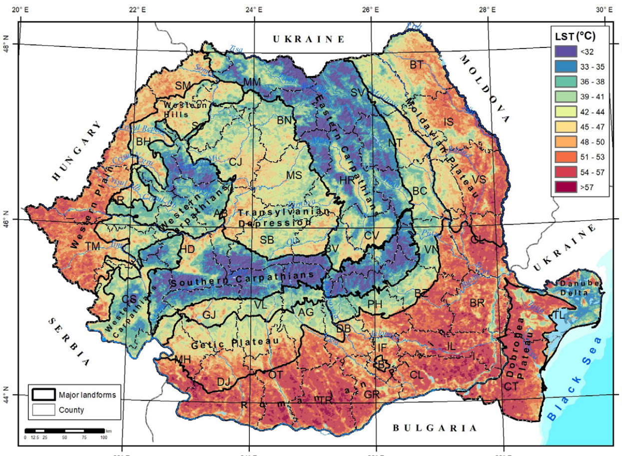

Figura 8. LST maximum values during heatwaves 2000-2025

The 24 July 2007 event was characterized by very high LST over Dobrogea, the Bărăgan Plain, and the Moldavian Plateau, whereas the August 2012 heatwave produced the largest spatial concentration of exceptionally high LST across central Romania, despite the highest absolute LST values remaining concentrated in the southern lowlands.

The selected event from July 2022 illustrates the pronounced warming over western Romania, while the July and August 2024 examples demonstrate the exceptional spatial extent of extreme LST simultaneously affecting southern, eastern, and western Romania. Comparable large-scale patterns were also recorded during the exceptional summer of 2025. Overall, satellite observations from the major heatwave years indicate that the most intense surface heating consistently occurred across the lowlands of southern and southeastern Romania, particularly within the Romanian Plain, Dobrogea, and the Bărăgan Plain, where LST locally exceeded 50°C. These findings confirm that the southern lowlands remain the region most exposed to extreme summer surface temperatures, while recent heatwaves have become progressively more spatially extensive, affecting increasingly larger areas of the country, including central and western Romania

Synoptic analysis of the landmark 2007 event highlights the physical footprint of extreme anticyclonic blocks. During the 15–25 July thermal wave, the advection of continental tropical air masses pushed afternoon surface temperatures past critical thresholds, triggering the first historical warm-season Red Code alert for the southern tier (Dolj, Olt, Teleorman, Giurgiu, and Ilfov counties). This institutional severity index aligns precisely with the MODIS overpass signatures (~10:30–12:10 UTC), which captured a contiguous radiometric core exceeding 40°C across the southern lowlands (Fig. S4).

Similarly, the macro-climatic shifts of August 2012 demonstrate severe land-surface feedback dynamics. During this event, the meteorological station network registered an absolute air temperature peak of 41.5°C in Bucharest (Filaret), breaking a multi-decadal record dating back to August 1945. The simultaneous satellite imagery validates this extreme atmospheric forcing, mapping expansive surface anomalies where radiometric LST consistently surpassed 50°C in the eastern and southern sectors during the initial wave (6–7 August) and localized values above 44°C extending into the Danube Valley and central tablelands during the secondary wave (23–26 August) (Fig. S4).

This compounding pattern of spatial expansion and increased frequency peaked during the 2024 warm season. June and August 2024 were documented as the hottest corresponding months since 1901, leading to an unprecedented administrative response with yellow, orange,

https://doi.org/10.5194/egusphere-2026-4415
Preprint. Discussion started: 11 August 2026

or red warnings active on 15 days in June, 20 days in July, and 22 days in August. Critically, the mid-July peak (15–17 July) marked the first synchronous nationwide Red Code deployment in Romanian meteorological history. The spatial manifestation of this extreme forcing is physically mapped by the MODIS layers, which delineate a continuous surface thermal footprint exceeding 50°C enveloping the entire Romanian Plain and Dobrogea Plateau, with extensive high-temperature cells invading the Moldavian Plateau and the Western Plain.

The **cumulative number of heatwave warning days** during 2006–2025 exhibits a clear regional concentration in southern Romania, particularly over the southern lowlands The highest totals were recorded in Dolj, Teleorman, Olt, Giurgiu, Ilfov, Bucharest-Ilfov region, and Călărași, followed by several neighbouring counties located within the Romanian Plain and Lower Danube Plain (Fig. S6). In all administrative units, yellow warnings constitute the largest share of warning days, indicating that most heatwave events were of moderate severity, whereas orange warnings contributed substantially to the cumulative totals.

In contrast, northern and central mountainous counties experienced substantially fewer warning days. This spatial pattern closely mirrors the distribution of maximum land surface temperatures and the Heat Vulnerability Index presented in the previous sections, confirming the greater susceptibility of the southern Romanian lowlands to prolonged heat stress (Fig S7).

The three warning categories display distinct spatial characteristics. **Yellow** warnings were the most frequent and affected almost the entire country, although their cumulative number was considerably higher in southern Romania than elsewhere (Fig. S7a).

Orange warnings were concentrated primarily across the southern and western lowlands, indicating a greater occurrence of more severe heatwave conditions in these regions (Fig. S7d). **Red** warnings were comparatively infrequent but showed a clear concentration in the Romanian Plain and Lower Danube Plain (Fig. S7g), emphasizing that the most extreme thermal events repeatedly affected the same geographical areas.

The maps of the longest consecutive warning sequences (Fig. S7b, S7e, and S7h) further demonstrate that southern counties experienced not only the highest number of warning days but also the longest uninterrupted heatwave episodes, indicating greater persistence of extreme thermal conditions.

The temporal distribution of the most persistent warning episodes also exhibits considerable regional variability. The **longest yellow-warning** sequences occurred during different years across Romania, reflecting the spatial heterogeneity of moderate heatwave events (Fig. S7c). In contrast, the longest orange-warning episodes were predominantly associated with the recent period (2021–2024), while the longest red-warning sequences occurred mainly during the exceptional summer of 2024 (Fig. S7i). Similarly, the year with the maximum consecutive heatwave warning days, irrespective of warning level, was 2024 for most counties in southern Romania, whereas northern and central regions reached their maximum persistence during earlier events, particularly 2007 and 2012 (Fig. S7k). Finally, the cumulative warning severity index (Fig. S7l), integrating the contribution of yellow, orange, and red warnings, identifies the Romanian Plain, the Lower Danube Plain, and the Bucharest metropolitan area as the regions experiencing the greatest overall heatwave burden during the study period.

The spatial distribution of **HVI** reveals pronounced regional differences in vulnerability to extreme heat across Romania (Fig. 9). The highest HVI values (0.60–0.80) are concentrated in the southern lowlands, with the **Bucharest** metropolitan area emerging as the most prominent hotspot of heat vulnerability. High vulnerability (0.45–0.60) extends across large sectors of the Romanian Plain and Lower Danube Plain, indicating areas where intense thermal exposure coincides with less favourable socioeconomic conditions and reduced adaptive capacity. Moderate HVI values (0.30–0.45) characterize extensive areas of western and eastern Romania, whereas the lowest vulnerability levels (<0.30) are predominantly associated with the

https://doi.org/10.5194/egusphere-2026-4415
Preprint. Discussion started: 11 August 2026

Carpathian Mountains and other high-altitude regions. This spatial pattern closely reflects the combined influence of physiographic conditions, settlement distribution, and heat exposure, emphasizing the strong contrast between densely populated lowlands and the cooler mountainous regions.

Overall, the results identify **southern Romania** as the area **most susceptible** to heat-related impacts, highlighting the need for targeted adaptation and mitigation measures in these regions. The strong spatial agreement between warning frequency, warning persistence, cumulative warning severity, maximum land surface temperatures during heatwaves days, and the HVI demonstrates that southern Romania has experienced a systematic intensification of heatwave conditions over the last two decades. These findings identify the Romanian Plain, (including the Bucharest metropolitan area) as the country's principal hotspot of heat-related risk and emphasize the growing persistence and severity of extreme summer conditions in recent years.

The **distribution** of the Romanian **population** across the **HVI** classes indicates that a considerable share of the population is exposed to elevated heat vulnerability (Fig. 10). More than 3 million inhabitants (approximately 16.5% of the national population) fall within the High and Very High HVI classes (0.45–0.80), whereas fewer than 300,000 people (approximately 1.2% of the national population) belong to the Very Low vulnerability class (0–0.15).

Although the largest absolute number of elderly residents occurs in the Moderate HVI class (1.75 million), the relative contribution of older adults to the total population increases with heat vulnerability, reaching 22.34% in the High HVI class before slightly declining to 18.82% in the Very High class (Fig. 10D–E).

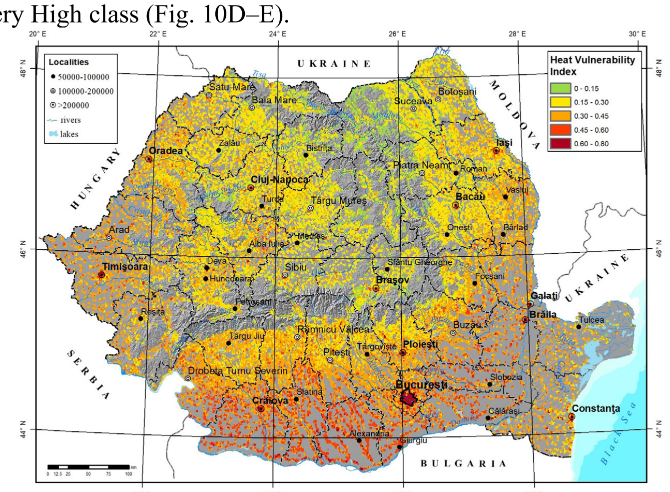

Figure 9. Spatial distribution of the population-grid Heat Vulnerability Index (HVI) across Romania

The progressive increase in HVI is accompanied by a corresponding increase in thermal exposure and warning severity. Mean land surface temperature (LST) rises from 36.71°C in the Very Low HVI class to 50.8°C in the High class, respectively 49°C in the Very High class, while the weighted warning severity index more than doubles, increasing from 113.6 to 465.6. These results indicate a strong positive relationship between heat vulnerability, thermal conditions, and the cumulative severity of heatwave warnings. Population age structure shows a slight increase across the HVI classes. The proportion of residents aged 65 years or older rises from 18.40% in the Very Low class to a maximum of 22.83% in the High class, before decreasing slightly to 18.82% in the Very High class. Overall, the results suggest a modest tendency for higher-vulnerability areas to contain a relatively larger share of elderly residents, although the differences among classes are not pronounced.

https://doi.org/10.5194/egusphere-2026-4415
Preprint. Discussion started: 11 August 2026

Consequently, the highest HVI classes combine elevated thermal exposure, more severe heatwave conditions, and a greater concentration of elderly residents, identifying these areas as priority targets for heat adaptation and public health interventions.

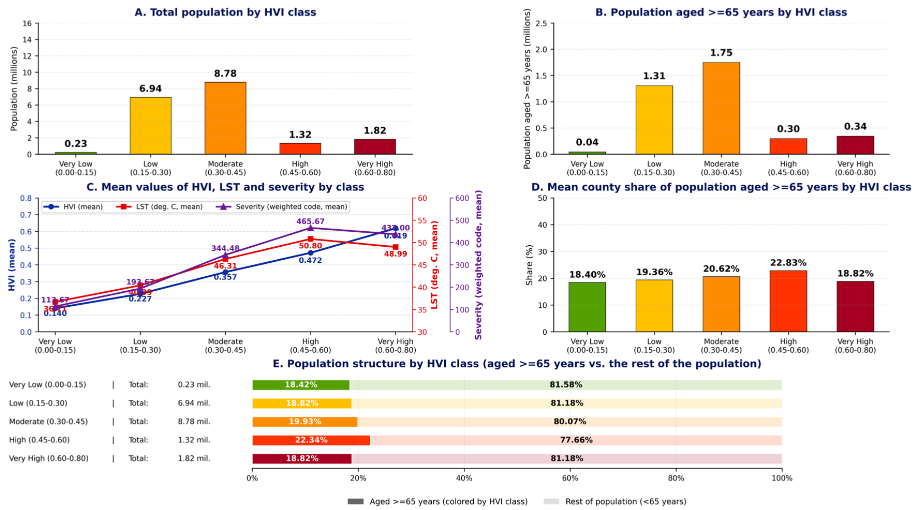

Figure 10. Heat Vulnerability Index (HVI) statistics by class (fixed thresholds: 0-0.15; 0.15-0.30; 0.30-0.45; 0.45-0.60; 0.60-0.80)

The county-level Heat Vulnerability Index reveals a pronounced spatial concentration of heat-related vulnerability in southern Romania (Fig. 11). Bucharest exhibits the highest mean HVI (0.61), followed by Teleorman, Dolj, Olt, Călărași, Giurgiu, and Ialomița, confirming the Romanian Plain as the country's principal hotspot of heat vulnerability. Overall, the 18 highest-ranked counties are predominantly located in southern and southeastern Romania, where elevated land surface temperatures coincide with high population density, increased heatwave severity, and a relatively large proportion of elderly residents.

The decomposition of HVI into its three main components demonstrates that heat vulnerability is driven by the combined effects of hazard, exposure, and demographic vulnerability, although their relative contribution varies among counties. **Bucharest** and **Ilfov** are primarily characterized by exceptionally **high exposure** resulting from very high population density, whereas counties such as Teleorman, Olt, and Dolj combine elevated thermal hazard with a comparatively larger elderly population. This confirms that high vulnerability does not result from a single factor but from the interaction of climatic and socioeconomic conditions.

The relationship between thermal hazard and the proportion of residents aged 65 years further highlights distinct vulnerability profiles. Counties such as **Teleorman** and **Olt** combine **high thermal hazard** with a large elderly population, whereas **Bucharest** is distinguished by the **highest exposure** despite a lower proportion of elderly residents. Conversely, several central counties exhibit comparatively low hazard and lower vulnerability, emphasizing the strong regional contrast in heat-related risk across Romania.

The standardized comparison of HVI components confirms the predominance of southern counties, which consistently display above-average values for hazard, land surface temperature, warning severity, and overall HVI. Population exposure reaches its highest values in Bucharest and Ilfov, whereas demographic vulnerability is particularly pronounced in Teleorman and Olt. These differences illustrate the heterogeneous mechanisms through which heat vulnerability develops across Romania.

https://doi.org/10.5194/egusphere-2026-4415
Preprint. Discussion started: 11 August 2026

The population analysis indicates that **3.15 million inhabitants** (16.5% of Romania's population) live in areas classified as having **high heat vulnerability** (HVI > 0.45). Bucharest alone accounts for approximately 1.82 million inhabitants within this class, representing 9.5% of the national population, followed by Dolj, Olt and Teleorman counties.

These findings emphasize the substantial concentration of heat-related risk within the southern urban and lowland regions and highlight the importance of prioritizing adaptation measures in these areas. Heat vulnerability is greatest in the southern Romanian lowlands and progressively decreases towards the central and mountainous regions.

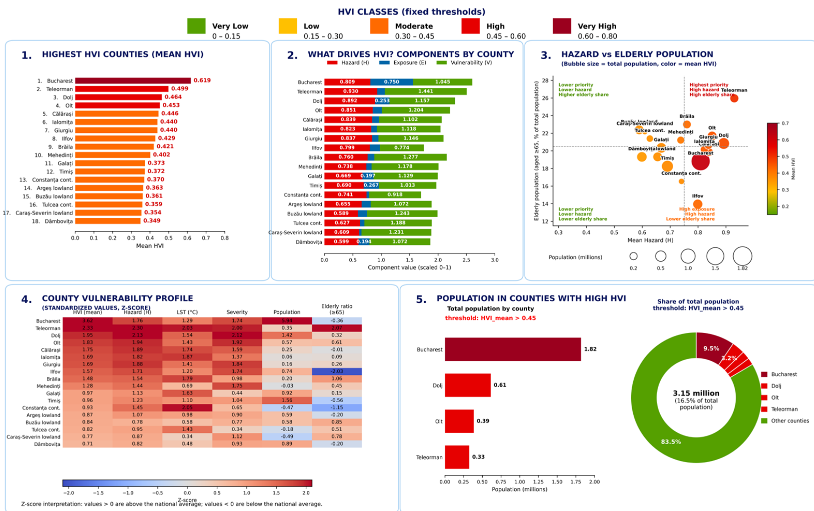

Figure 11. Heat Vulnerability Index (HVI) by county

The spatial distribution of **household air conditioning** (AC) ownership broadly follows this pattern, with the highest shares observed in Bucharest, Constanța, and Timiș, whereas considerably lower AC penetration characterizes counties such as Harghita, Covasna, Suceava, and Maramureș. As shown in Figure 12, average household AC ownership increases consistently with HVI, rising from 6.0% in counties classified as having low vulnerability to 28.9% in those with very high vulnerability (Fig. S8). This spatial correspondence indicates that residential cooling has been adopted more extensively in areas exposed to greater heat stress. Nevertheless, even within the highest HVI class, fewer than one-third of households are equipped with AC. Moreover, several counties with high or very high heat vulnerability, including Teleorman, Olt, Dolj, Giurgiu, and Călărași, still exhibit relatively modest AC ownership, suggesting that adaptive capacity remains insufficient in some of the regions most exposed to extreme summer heat.

https://doi.org/10.5194/egusphere-2026-4415
Preprint. Discussion started: 11 August 2026

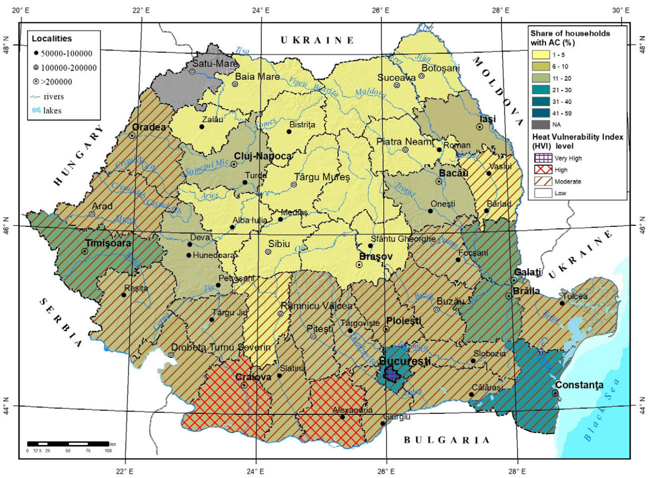

Figure 12. Spatial relationship between household air conditioning (AC) availability and the Heat Vulnerability Index (HVI) across Romania.

Discussions

The Heat Vulnerability Index is a composite indicator designed to identify populations and areas most susceptible to the adverse impacts of extreme heat. Rather than relying solely on temperature, HVI integrates multiple environmental, demographic, health, and socioeconomic indicators to provide a spatial representation of heat-related risk. Although individual methodologies differ, most HVI frameworks are based on the conceptual approach proposed by the Intergovernmental Panel on Climate Change (IPCC), which defines vulnerability as the interaction between hazard (or exposure), sensitivity, and adaptive capacity (Reid et al., 2009; Bao et al., 2015; Niu et al., 2021; Qian and Liu, 2025).

HVI has become one of the most widely used approaches for identifying populations and regions at risk from extreme heat (Bao et al., 2015). Most HVI studies conceptualize vulnerability as the interaction between three main dimensions: heat exposure (hazard), population sensitivity, and adaptive capacity, although the specific indicators and weighting methods vary considerably among studies (Niu et al., 2021; Qian et al., 2025).

Previous studies have predominantly focused on urban environments and metropolitan areas, where HVI has been derived by combining remotely sensed thermal indicators with demographic and socioeconomic variables. Common exposure indicators include land surface temperature (LST), urban heat island intensity, vegetation indices (NDVI), impervious surfaces, or land-cover characteristics obtained from Landsat or MODIS imagery, whereas sensitivity and adaptive-capacity indicators typically include population density, age structure, income, education, housing conditions, and access to cooling (Inostroza et al., 2016).

Li et al. (2024) argued that one of the main limitations of current HVI studies is the lack of standardized methodologies, inconsistent indicator selection, reliance on administrative units, and limited temporal coverage. They proposed that future heat vulnerability assessments should integrate long-term remote sensing observations, grid-scale spatial analysis, and continuous monitoring to improve robustness and support climate adaptation planning.

Reid et al. (2009) demonstrated that heat vulnerability is determined not only by thermal exposure but also by a combination of demographic, socioeconomic and environmental characteristics. Their Heat Vulnerability Index incorporated variables describing age structure, education, poverty, social isolation, diabetes prevalence, vegetation cover and household air conditioning availability, highlighting that the highest heat-related mortality risk occurs where high temperatures coincide with socially vulnerable populations and limited adaptive capacity.

https://doi.org/10.5194/egusphere-2026-4415
Preprint. Discussion started: 11 August 2026

The inclusion of household air conditioning availability from the recent census database in the present study was integrated specifically as a macro-scale operational proxy for technological adaptive capacity. In heat vulnerability architecture, air conditioning represents the most direct spatial baseline for indoor thermal regulation and active heat-stress mitigation. However, to avoid ecological fallacies stemming from the inherent scale mismatch between the administrative data and the physical climate parameters, these statistics were treated strictly as a macro-regional contextual overlay at the county level rather than being integrated directly into the high-resolution pixel calculations. This strategic decoupling prevents the spatial smoothing of localized grid variations while still providing public health administrators with a crucial, aggregate overview of where high regional physical vulnerability intersects with systemic deficits in residential cooling infrastructure across Romania.

Unlike most previous HVI studies, which evaluate vulnerability for individual cities or metropolitan regions using one or several satellite images representing specific heatwave events, the present study adopts a long-term national-scale approach. Heat exposure was characterized using a 26-year MODIS LST archive (2000–2025), combined with the complete record of official Romanian heatwave warnings and population-based indicators. The analysis was performed on a population-grid framework, enabling a spatially continuous assessment of heat vulnerability across the entire territory of Romania rather than within a single urban area.

To our knowledge, this represents the first national-scale Heat Vulnerability Index developed for Romania using a 26-year MODIS LST climatology combined with official operational heatwave warnings and 1-km population-grid data.

Direct spatial validation of the computed Heat Vulnerability Index using long-term, geo-referenced epidemiological datasets—such as daily cause-specific mortality or emergency ambulance dispatches—was constrained by institutional data-sharing limitations and the historical unavailability of continuous, fine-scale medical registries tracking a multi-decadal timeline across Romania. Consequently, the index developed in this study is explicitly designed to function as a macro-scale, predictive screening tool to assist public health resource allocation, rather than an empirical epidemiological model. Despite this data constraint, the spatial distribution of the high and very high vulnerability classes provides robust proxy validation, as these areas directly overlap with regions documented in historical literature to bear the highest health impacts during severe thermal blocks. For instance, the pronounced vulnerability hotspots identified along the southern and western lowlands, as well as major metropolitan areas like Bucharest, strongly coincide with established regional literature detailing peak spikes in cardiovascular stress, heat-related morbidity, and excess urban mortality during past extreme heatwaves. This structural alignment confirms that even in the absence of direct, fine-scale historical health data, combining satellite-derived exposure with standardized demographic indicators yields a highly reliable geographic baseline for proactive climate adaptation planning.

This extreme concentration of vulnerability in the capital city empirically highlights the "urban heat risk penalty," where high population density synergistically amplifies satellite-derived surface thermal anomalies. This spatial pattern aligns closely with recent microclimatic findings in southern European metropolises, such as Athens and Budapest, where compact high-rise urban fabrics exhibit a severe deficit in thermal regulation compared to their rural peripheries (Constantinou et al., 2024; Kerényi et al., 2025). The fact that the metropolitan population is structurally locked into the highest HVI tiers confirms that urban vulnerability in Romania is primarily driven by exposure magnitude rather than localized demographic sensitivity variations alone. This critical structural imbalance demands immediate, targeted macro-scale green infrastructure intervention to break the surface energy retention loop within the capital's densest residential sectors.

https://doi.org/10.5194/egusphere-2026-4415
Preprint. Discussion started: 11 August 2026

Another distinctive aspect of this study is the explicit incorporation of the operational heatwave warning system into the HVI framework. While most published indices rely primarily on thermal variables derived from satellite observations or air temperature records, the proposed methodology integrates the cumulative severity and persistence of official meteorological warnings together with satellite-derived LST and demographic indicators. Consequently, the resulting HVI reflects not only long-term thermal exposure but also the actual operational warning conditions experienced by the population during heatwave events.

The observed agreement between HVI, long-term MODIS LST, heatwave warning severity, and the spatial distribution of elderly population provides indirect validation of the proposed index. Counties classified as highly vulnerable consistently exhibited higher surface temperatures, more persistent and severe heatwave warnings, and a greater concentration of elderly residents, suggesting that the adopted framework successfully captures both the physical and socioeconomic dimensions of heat-related vulnerability.

Similar to Adnan et al. (2024), who incorporated long-term MODIS-derived land surface temperature into a Heat Vulnerability Index (HVI) framework, our study demonstrates the value of satellite-derived LST for identifying spatial patterns of heat exposure at the national scale. In both studies, areas characterized by persistently elevated LST generally coincide with the highest levels of heat vulnerability.

Satellite-derived LST products are inherently limited by **cloud cover**, as reliable surface temperature retrievals are only available under clear-sky conditions. Consequently, evaluating cloud cover during heatwave-warning days provides an important assessment of the potential influence of cloud-related data gaps on the LST climatology presented in this study.

Cloud cover during heatwave-warning days was analysed to provide additional context for the observed land surface temperature patterns. As shown in Figure S9, heatwave events in Romania occurred predominantly under low-cloud conditions, with an average cloud cover of **28.5%** and a median of 22.6%. The positive skewness of the distribution indicates that highly cloudy heatwave days were relatively uncommon.

Monthly differences were relatively small, although August exhibited a slightly lower median cloud cover than June and July, suggesting that late-summer heatwaves were generally associated with clearer atmospheric conditions. This is consistent with the higher land surface temperatures observed during August, when reduced cloudiness allows greater incoming solar radiation and enhanced surface heating.

The annual boxplots indicate considerable interannual variability in cloud cover during heatwave events, with no clear long-term trend over the study period. Nevertheless, recent years (2022–2025) show a wider range of cloud cover values, reflecting the occurrence of heatwaves under both clear and moderately cloudy conditions.

The heatmap further demonstrates that the majority of heatwave-warning days were associated with cloud cover below 40–50%, whereas events exceeding 70% cloud cover occurred only occasionally. These results suggest that most heatwaves developed under conditions favourable for strong surface heating, while only a small proportion of events were accompanied by substantial cloudiness (Figure S9).

Although MODIS provides a consistent long-term dataset, the 1-km spatial resolution does not capture fine-scale urban thermal heterogeneity, particularly within large cities. Future studies should integrate higher-resolution Landsat or ECOSTRESS observations to better characterize intra-urban heat exposure.

Future work will explicitly address the multi-dimensional complexity of heat stress by expanding the purely satellite-derived framework. While the current 1-km Heat Vulnerability Index (HVI) provides a robust operational screening baseline, incorporating high-resolution spaceborne indicators of adaptive capacity and bioclimatic comfort remains a priority. Subsequent iterations of the model will integrate MODIS 16-day maximum value composite

https://doi.org/10.5194/egusphere-2026-4415
Preprint. Discussion started: 11 August 2026

NDVI (MOD13A2) and Evapotranspiration (MOD16A2) products directly into the baseline pixel calculations. This will transition the adaptive capacity component from coarse, administrative county-level air conditioning statistics to continuous, grid-scale metrics of urban green infrastructure and canopy-driven evapotranspirative cooling. Furthermore, to capture the synergistic effects of humidity and nocturnal thermal persistence—critical drivers of cardiovascular morbidity—future developments will incorporate MODIS night-time LST retrievals alongside column atmospheric water vapor profiles (MOD07_L2) to compute spatialized Satellite Temperature-Humidity Indices (S-THI). Finally, to overcome the systematic clear-sky bias inherent to thermal infrared remote sensing during humid, transitional heatwaves, localized temporal interpolation and neighboring-pixel weight algorithms will be deployed within the Google Earth Engine workflow. This comprehensive expansion will allow the HVI to evolve from a static vulnerability screening tool into a dynamic, cloud-corrected biometeorological early-warning framework.

Conclusions

This study provides the first long-term, national-scale assessment of heat hazard and heat vulnerability in Romania by integrating a 26-year MODIS Land Surface Temperature (LST) archive (2000–2025), official heatwave warnings, and population-grid demographic data within a unified Heat Vulnerability Index (HVI). The proposed framework combines satellite observations with operational meteorological information, allowing both the thermal intensity of heatwaves and the spatial distribution of vulnerable populations to be evaluated simultaneously.

The results demonstrate a clear intensification of summer thermal conditions across Romania during the study period. August exhibited the strongest warming trend (1.76°C decade^{-1}), followed by July (0.82°C decade^{-1}), while seasonal (JJA) warming reached 0.84 °C decade^{-1} across almost the entire country. The hottest summers were recorded in 2025, 2024, 2012 and 2007, whereas July 2007 remained the month with the highest mean LST (35.4°C). Recent summers (2021–2025) were characterized not only by higher temperatures but also by substantially longer and more persistent heatwave episodes.

The spatial analyses consistently identified the Romanian Plain, the Lower Danube Plain, Dobrogea and the western lowlands as the principal hotspots of extreme surface heating. During the most severe events, maximum LST frequently exceeded 50°C, while mountainous regions remained substantially cooler owing to the combined influence of altitude and land cover. The strong relationship between MODIS-derived LST and maximum air temperature ($R^2 = 0.68$) further confirms the suitability of satellite observations for large-scale heatwave monitoring.

The integration of long-term LST, cumulative heatwave-warning severity, population density and the proportion of elderly residents revealed pronounced regional differences in heat vulnerability. The highest HVI values were concentrated in southern Romania, particularly within the Bucharest metropolitan area and the surrounding counties of Teleorman, Dolj, Olt, Călărași, Giurgiu and Ialomița. Approximately 3.15 million inhabitants (16.5% of Romania's population) live in areas classified as having high heat vulnerability, emphasizing the substantial concentration of heat-related risk within densely populated southern lowlands.

The comparison between household air-conditioning availability and HVI indicates that adaptive capacity remains insufficient in many of the regions experiencing the greatest thermal stress. Although air-conditioning ownership increases with vulnerability, fewer than one-third of households in the highest HVI class are equipped with air-conditioning systems, and several counties characterized by high HVI still exhibit relatively limited cooling capacity. These findings suggest that socioeconomic adaptation has not kept pace with the rapid increase in heat exposure.

https://doi.org/10.5194/egusphere-2026-4415
Preprint. Discussion started: 11 August 2026

From a methodological perspective, this study demonstrates the added value of combining long-term satellite observations with operational meteorological warnings and demographic information within a population-grid framework. Unlike previous studies focused primarily on urban environments or individual heatwave events, the proposed approach provides a spatially continuous national assessment of heat vulnerability that can be readily updated using routinely available satellite and meteorological products.

Overall, the results indicate that southern Romania has become increasingly exposed to more frequent, persistent and intense heatwaves, while demographic characteristics further amplify vulnerability in many counties. The proposed Heat Vulnerability Index provides a practical tool for identifying priority areas for climate adaptation, public-health interventions and heat-risk management, supporting evidence-based decision making under future climate warming.

The integration of long-term Earth Observation data, operational meteorological warnings, and population-based indicators provides a robust and transferable framework for identifying heat-vulnerability hotspots and supporting evidence-based climate adaptation, public health planning, and sustainable territorial management in Romania and other regions facing increasing heat stress.

In conclusion, the 1-km Heat Vulnerability Index (HVI) developed in this study transcends theoretical mapping, establishing an empirical blueprint for targeted climate resilience in Romania. By bridging the operational gap between satellite-derived macro-climatic hazards and fine-scale human demography, this framework provides public health authorities, urban planners, and emergency services with an actionable diagnostic tool. As summer thermal extremes continue to accelerate in both frequency and severity, as demonstrated by the record-breaking events of 2024 and 2025, the proactive spatial allocation of resources - ranging from localized green infrastructure expansion to the optimization of emergency medical dispatches - will become paramount. This study delivers the geographical baseline necessary to transition from reactive crisis management to evidence-based, preventative climate adaptation planning at a nationwide scale.

Author Contributions

All authors contributed to the study conception and design. Material preparation, data collection, and satellite imagery processing were performed by C.A., D.M. and V.C. The methodology, development of the Heat Vulnerability Index (HVI), and statistical analyses were conducted by C.A., M.N. and F.G. The first draft of the manuscript was written by C.A. and A.I., and all authors commented on previous versions of the manuscript. All authors read and approved the final manuscript.

Funding

This work was supported by a grant of the Ministry of Research, Innovation and Digitization, CCCDI-UEFISCDI, project number PN-IV-P6-6.3-SOL-2024-2-0248, within PNCDI IV.

Data availability

The daily MODIS Land Surface Temperature data were accessed and processed using the Google Earth Engine platform. The Terra MODIS MOD11A1 Version 6.1 image collection (Earth Engine identifier: MODIS/061/MOD11A1) was used for 2000–2001 and is publicly available at https://developers.google.com/earth-engine/datasets/catalog/MODIS_061_MOD11A1. The Aqua MODIS MYD11A1 Version 6.1 image collection (Earth Engine identifier: MODIS/061/MYD11A1) was used for 2002–2025

https://doi.org/10.5194/egusphere-2026-4415
Preprint. Discussion started: 11 August 2026

and is publicly available at *https://developers.google.com/earth-engine/datasets/catalog/MODIS_061_MYD11A1*.

The original products are provided by the NASA Land Processes Distributed Active Archive Center and are referenced by https://doi.org/10.5067/MODIS/MOD11A1.061 and https://doi.org/10.5067/MODIS/MYD11A1.061.

The 2021 population grid data, including total population and population aged 65 years and over at 1 km² resolution, are publicly available from Eurostat GISCO at https://ec.europa.eu/eurostat/web/gisco/geodata/population-distribution/population-grids. County-level census data on household air-conditioning availability are available from the final results of the Romanian Population and Housing Census 2021 at https://www.recensamantromania.ro/rezultate-rpl-2021/rezultate-definitive/.

The daily gridded maximum air temperature data are available from the Romanian National Meteorological Administration through the Romanian Open Data Portal at https://data.gov.ro/dataset/date-meteorologice-zilnice-gridate.

The official yellow-, orange-, and red-level heat-warning records used in this study were obtained from the operational archive of the Romanian National Meteorological Administration (ANM). The harmonized historical warning archive is not publicly available because it is an institutional data product whose dissemination and redistribution are subject to ANM data-access rules and prior institutional authorization. Consequently, the authors are not authorized to independently deposit these data in a public repository. Requests for access may be submitted to the corresponding author (anisoara.irimescu@meteoromania.ro) or to the Romanian National Meteorological Administration (relatii@meteoromania.ro; https://www.meteoromania.ro/). Access may be granted upon request, subject to institutional approval.

Conflict of Interest

The authors have no relevant financial or non-financial interests to disclose.

References

Adnan, M. S. G., Kabir, I., Hossain, M. A., Chakma, S., Tasneem, S. N., Saha, C. R., Hassan, Q. K., and Dewan, A.: Heatwave vulnerability of large metropolitans in Bangladesh: An evaluation, Geomatica, 76, 100020, https://doi.org/10.1016/j.geomat.2024.100020, 2024.

Antonescu, B., Ene, D., Boldeanu, M., Andrei, S., Marmureanu, L., Marin, C., and Pirloaga, R.: Future changes in heatwaves characteristics in Romania, Theor. Appl. Climatol., 153, 525–538, https://doi.org/10.1007/s00704-023-04412-5, 2023.

Antonescu, B. and Ioniță, M.: The intensification of compound hot-dry extremes in Eastern Europe: Observational trends and synoptic driving mechanisms, Atmos. Res., 302, 107314, https://doi.org/10.1016/j.atmosres.2024.107314, 2024.

Bao, J., Li, X., and Yu, C.: The construction and validation of the Heat Vulnerability Index, a review, Int. J. Environ. Res. Public Health, 12, 7220–7234, https://doi.org/10.3390/ijerph120707220, 2015.

Barriopedro, D., Fischer, E. M., Luterbacher, J., Trigo, R. M., and Garcia-Herrera, R.: The hot summer of 2010: Redrawing the temperature record map of Europe, Science, 332, 220–224, https://doi.org/10.1126/science.1201224, 2011.

Barbu, N., Georgescu, F., Stefanescu, V., and Stefan, S.: Large-scale mechanisms responsible for heat waves occurrence in Romania, Rom. J. Phys., 59, 1109–1126, 2014.

Bojariu, R., Chitu, Z., Dascalu, S. I., Gothard, M., Velea, L. F., Burcea, R., Dumitrescu, A., Burcea, S., Apostol, L., Amihaesei, V., Marin, L., Craciunescu, V. S., Irimescu, A., Matreata, M., Nita, A., and Birsan, M. V.: Schimbarile climatice – de la bazele fizice la riscuri si adaptare, 2nd edn., Editura Printech, Bucharest, Romania, 341 pp., ISBN 978-606-23-1224-4, 2021.

Bunting, E. L., Tolmanov, V., and Keellings, D.: What is a heat wave: A survey and literature synthesis of heat wave definitions across the United States, PLOS Clim., 3, e0000468, https://doi.org/10.1371/journal.pclm.0000468, 2024.

Buscail, C., Upegui, E., and Viel, J. F.: Mapping heatwave health risk at the community level for public health action, Int. J. Health Geogr., 11, 38, https://doi.org/10.1186/1476-072X-11-38, 2012.

https://doi.org/10.5194/egusphere-2026-4415
Preprint. Discussion started: 11 August 2026

Cheval, S., Amihaesei, V. A., Dumitrescu, A., Micu, D. M., and Smau, R. I.: Observed variability and future projections of urban heatwaves in Romania, Int. J. Climatol., 45, e8714, https://doi.org/10.1002/joc.8714, 2025.

Cheval, S., Micu, D., Dumitrescu, A., and Sîrbu, C.: High-resolution modeling of urban heat island dynamics in Romania during extreme synoptic events, Urban Clim., 59, 102180, https://doi.org/10.1016/j.uclim.2024.102180, 2025.

Constantinou, A., Katavoutas, G., and Founda, D.: Evaluating the urban heat risk penalty in compact Mediterranean cities: Spatial infrastructure feedbacks and thermal discomfort dynamics in Athens, Int. J. Biometeorol., 68, 712–729, https://doi.org/10.1007/s00484-024-02641-x, 2024.

Croitoru, A. E., Piticar, A., Ciupertea, A. F., and Rosca, C. F.: Changes in heat waves indices in Romania over the period 1961–2015, Global Planet. Change, 146, 109–121, https://doi.org/10.1016/j.gloplacha.2016.08.016, 2016.

Croitoru, A.-E., Piticar, A., Sfîcă, L., Harpa, G. B., Roşca, C. F., Tudose, T., Horvath, C., Minea, I., Ciupertea, F. A., and Scripcă, A. S.: Fenomene climatice și hidrologice extreme în România, Editura Academiei Române, Bucharest, Romania, 359 pp., ISBN 978-973-27-2833-8, 2018.

Dima, V., Georgescu, F., Irimescu, A., and Mihailescu, D.: Valuri de caldura in Romania, Editura Printech, Bucharest, Romania, 89 pp., ISBN 978-606-23-0666-3, 2016.

Dousset, B., Gourmelon, F., Laaidi, K., Zeghnoun, A., Giraudet, E., Bretin, P., Mauri, E., and Vandentorren, S.: Satellite monitoring of summer heat waves in the Paris metropolitan area, Int. J. Climatol., 31, 313–323, https://doi.org/10.1002/joc.2222, 2011.

EUMETNET: Meteoalarm – European Multi-services Meteorological Awareness (EMMA), https://meteoalarm.org, last access: 8 July 2026, 2024.

Gabrian, A., Sfîcă, L., and Ichim, P.: Microclimatic disruptions and nighttime thermal retention profiles across major urban fabrics in Romania, Theor. Appl. Climatol., 159, 445–462, https://doi.org/10.1007/s00704-024-05112-w, 2025.

Gusso, A., Ducati, J. R., Veronez, M. R., Sommer, V., and Gonzaga, L. S. J.: Monitoring heat waves and their impacts on summer crop development in Southern Brazil, Agric. Sci., 5, 353–364, https://doi.org/10.4236/as.2014.54037, 2014.

Inostroza, L., Palme, M., and de la Barrera, F.: A Heat Vulnerability Index: Spatial patterns of exposure, sensitivity and adaptive capacity for Santiago de Chile, PLOS ONE, 11, e0162464, https://doi.org/10.1371/journal.pone.0162464, 2016.

Ionita, M., Dima, V., Nagavciuc, V., and Vaideanu, P.: The extraordinary 2020 summer heatwave in Romania and its metropolitan areas, Theor. Appl. Climatol., 145, 1145–1158, https://doi.org/10.1007/s00704-021-03681-y, 2021.

Ionita, M., Vaideanu, P., Antonescu, B., Roibu, C., Ma, Q., and Nagavciuc, V.: Examining the Eastern European heatwave of 2023 from a long-term perspective: The role of natural variability vs. anthropogenic factors, EGUsphere [preprint], https://doi.org/10.5194/egusphere-2024-1207, 2024.

Ionita, M., Nagavciuc, V., and Scholz, P.: The unprecedented 2024 summer heatwave in Eastern Europe from a long-term climatological perspective, Int. J. Climatol., 45, 890–905, https://doi.org/10.1002/joc.8642, 2025.

Kerényi, A., Pongrácz, R., and Bartholy, J.: High-resolution satellite assessment of heatwave vulnerability and metropolitan thermal stress patterns in Central-Eastern Europe, Clim. Serv., 37, 100452, https://doi.org/10.1016/j.cliser.2024.100452, 2025.

Li, F., Yigitcanlar, T., Nepal, M., Thanh, K. N., and Dur, F.: A novel urban heat vulnerability analysis: Integrating machine learning and remote sensing for enhanced insights, Remote Sens., 16, 3032, https://doi.org/10.3390/rs16163032, 2024.

Marasoiu, D.: Fenomene climatice extreme: valuri de caldura si de frig in regiunile extracarpatice romanesti, PhD thesis, Institutul de Geografie al Academiei Române, Bucharest, Romania, 2015.

Martins, J. P. A., Caetano, S., Pereira, C., Dutra, E., and Cardoso, R. M.: A satellite view of the exceptionally warm summer of 2022 over Europe, Nat. Hazards Earth Syst. Sci., 24, 1501–1520, https://doi.org/10.5194/nhess-24-1501-2024, 2024.

Nagavciuc, V., Scholz, P., and Ionita, M.: Hotspots for warm and dry summers in Romania, Nat. Hazards Earth Syst. Sci., 22, 1347–1369, https://doi.org/10.5194/nhess-22-1347-2022, 2022.

National Institute of Statistics (INS): Romanian Population and Housing Census 2021 (RPL2021), county-level housing equipment data, https://recensamantromania.ro/rezultate-rpl-2021/rezultate-definitive/, last access: 10 May 2026, 2021.

Niu, Y., Li, Z., Gao, Y., and Liu, X.: A systematic review of the development and validation of the Heat Vulnerability Index: Major factors, methods, and spatial units, Curr. Clim. Change Rep., 7, 87–97, https://doi.org/10.1007/s40641-021-00173-3, 2021.

Qian, Y. and Liu, T.: Heat vulnerability assessment: A systematic review of critical metrics, Clim. Serv., 39, 100526, https://doi.org/10.1016/j.cliser.2025.100526, 2025.

https://doi.org/10.5194/egusphere-2026-4415
Preprint. Discussion started: 11 August 2026

Reid, C. E., O'Neill, M. S., Gronlund, C. J., Brines, S. J., Brown, D. G., Diez-Roux, A. V., and Schwartz, J.: Mapping community determinants of heat vulnerability, Environ. Health Perspect., 117, 1730–1736, https://doi.org/10.1289/ehp.0900683, 2009.

Romania Heat Atlas: Urban Heat Stress, Heatwave Dynamics, and Public Health Risk Assessment Framework for Romania (1940–present), https://heat-atlas.ro, last access: 8 July 2026, 2026.

Romanian National Meteorological Administration (ANM): ANM archive: Heat-warning data repository snapshot, 2025.

Sfica, L., Croitoru, A. E., Iordache, I., and Ciupertea, A. F.: Synoptic conditions generating heat waves and warm spells in Romania, Atmosphere, 8, 50, https://doi.org/10.3390/atmos8030050, 2017.

Tucci, M., Pigaiani, C., Freire, S., and Batista, F.: JRC-ESTAT Census Dwelling Grid 2021, European Commission, Joint Research Centre [data set], https://doi.org/10.2905/JRC.1NNF45G, 2026.

WMO: Guidelines on the definition and monitoring of extreme weather and climate events, WMO-No. 1203, World Meteorological Organization, Geneva, Switzerland, 43 pp., https://wmo.int, last access: 8 July 2026, 2018.

WMO and WHO: Heatwaves and Health: Guidance on Warning-System Development, WMO-No. 1142, World Meteorological Organization and World Health Organization, Geneva, Switzerland, 107 pp., https://wmo.int, last access: 8 July 2026, 2015.

Zaitchik, B. J., Macalady, A. K., Bonneau, L. R., and Smith, R. B.: Europe's 2003 heat wave: A satellite view of impacts and land–atmosphere feedbacks, Int. J. Climatol., 26, 743–769, https://doi.org/10.1002/joc.1280, 2006.

Zoran, M., Savastru, D., Miclos, S., Tautan, M. N., and Baschir, L.: Multisensor satellite remote sensing data for heat waves assessment in metropolitan region, J. Optoelectron. Adv. M., 13, 1159–1166, https://joam.inoe.ro/articles/multisensor-satellite-remote-sensing-data-for-heat-waves-assessment-in-metropolitan-region/fulltext, last access: 16 July 2026, 2011.